

## High energy particle background at neutron spallation sources and possible solutions

N Cherkashyna<sup>1,9</sup>, K Kanaki<sup>1</sup>, T Kittelmann<sup>1</sup>, U Filges<sup>2</sup>, P Deen<sup>1</sup>, K Herwig<sup>3</sup>, G Ehlers<sup>4</sup>, G Greene<sup>5</sup>, J Carpenter<sup>6</sup>, R Connatser<sup>1</sup>, R Hall-Wilton<sup>1,7</sup>, P M Bentley<sup>1,8</sup>

<sup>1</sup>European Spallation Source ESS AB, 221 00 Lund, Sweden

<sup>2</sup>Paul Scherrer Institute, 5232 Villigen PSI, Switzerland

<sup>3</sup>Instrument and Source Division, Oak Ridge National Laboratory, Oak Ridge, TN, 37831, USA

<sup>4</sup>Quantum Condensed Matter Division, Oak Ridge National Laboratory, Oak Ridge, TN, 37831, USA

<sup>5</sup>Physics Division, Oak Ridge National Laboratory, Oak Ridge, TN, 37831, USA

<sup>6</sup>Argonne National Laboratory, Argonne, IL, 60439, USA

<sup>7</sup>Department of Electronics, Mid Sweden University, Sundsvall, Sweden

<sup>8</sup>Department of Physics and Astronomy, Uppsala University, 751 05 Uppsala, Sweden

E-mail: nataliia.cherkashyna@esss.se

**Abstract.** Modern spallation neutron sources are driven by proton beams  $\sim$  GeV energies. Whereas low energy particle background shielding is well understood for reactors sources of neutrons ( $\sim$ 20 MeV), for high energies (100s MeV to multiple GeV) there is potential to improve shielding solutions and reduce instrument backgrounds significantly. We present initial measured data on high energy particle backgrounds, which illustrate the results of particle showers caused by high energy particles from spallation neutron sources. We use detailed physics models of different materials to identify new shielding solutions for such neutron sources, including laminated layers of multiple materials. In addition to the steel and concrete, which are used traditionally, we introduce some other options that are new to the neutron scattering community, among which there are copper alloys as used in hadronic calorimeters in high energy physics laboratories. These concepts have very attractive energy absorption characteristics, and simulations predict that the background suppression could be improved by one or two orders of magnitude. These solutions are expected to be great benefit to the European Spallation Source, where the majority of instruments are potentially affected by high energy backgrounds, as well as to existing spallation sources.

<sup>9</sup> To whom any correspondence should be addressed.



## 1. Introduction

The European Spallation Source combines a powerful spallation source with the instrumental goal of being able to measure weak processes with cold neutrons. Whereas existing spallation sources are either short pulse (microsecond) or continuous, the ESS will be a “long pulse” source, of the order of a few milliseconds, with a low repetition rate. Despite the low repetition rate, an optimisation of the long pulse instrumentation favours measurements across frame boundaries – i.e. when the next proton pulse produces neutrons (neutrons from several pulses are present in the instrument) – on approximately 70% of the instrument suite. The data spike that can be detected as the next pulse arrives is a high energy physics phenomenon that has been called a “prompt pulse”, because those neutrons possess such high energy that they appear at virtually zero time-of-flight as measured by the neutron instruments. The “prompt-pulse” has been observed since the first days of neutron spallation sources. The issue about high energy background and the technical challenges, related to it, has been known since those times [1].

In this paper we will give an overview on how the ESS is aiming to reduce the backgrounds on the instruments, present some new shielding solutions, with particular emphasis on reducing the signal from high energy background. This is of particular importance, because although the data spike is generally small, it is sometimes comparable or 1 or 2 orders of magnitude stronger in intensity to the interesting, weak phenomena that the instruments are designed to measure at meV energies.

One example of the high energy background problem is the data measured on HYSPEC instrument, the hybrid spectrometer at the Spallation Neutron Source (SNS, Oak Ridge National Laboratory, USA). The background signal is discussed in HYSPEC technical and status reports [2-3]. The time-dependent signal has a count rate comparable to expected inelastic count rate in some regions of the time window [2]. The background is observed when the instrument shutter is open and closed; it is not significantly affected by the heavy beam shutter, and therefore the source of this signal is believed not to be the instrument's own beamline.

If it was possible to reduce the background signal by two orders of magnitude, the intrinsic background on HYSPEC would be at the level desired for polarized inelastic neutron scattering, for all of incident energies available. It is one of our conclusions that modifications to the shielding strategy may be the best option to reduce this background. The prompt pulse is accompanied by a long tail of fast neutron spectra; which is likely to be caused by energetic neutrons being moderated by instrument and it's surroundings.

Another evidence of the problem is the data measured at CNCS instrument, the cold neutron chopper spectrometer at the Spallation Neutron Source (SNS, Oak Ridge National Laboratory, USA), see figure 1.

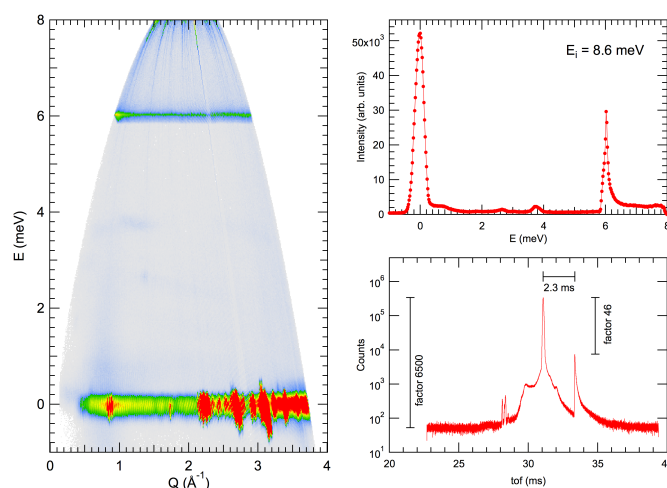


**Figure 1.** The bottom right shows the raw data as of time-of-flight, the prompt pulse peak is at 33.333 ms and the elastic line is at 31 ms. The top right shows how time-of-flight translates to energy transfer, with the prompt pulse at 6meV energy loss.

The left panel shows the data converted to the (Q,w) plane but otherwise uncorrected. The prompt pulse is at 33.333 because the instrument is in the third frame at this particular energy. The frame length is 16.667, SNS operates at 60Hz.

The high energy background does reduce the functionality of the neutron instruments, by increasing the noise-to-signal ratio. Typically, it causes a degradation in performance by forcing the instruments to discard a region in time-of-flight where the high energy background spike occurs. The spike is systematic – it is time correlated, and it is not a random error that reduces in relative size compared to the measured signal. Attempts to subtract this background have proven to be unsatisfactory.

A prime candidate mechanism in the prompt pulse is the phenomenon of particle showers. These are the cascades of secondary particles produced by high energy particle interactions with dense matter. There are two different mechanisms of particle showers: electromagnetic and hadronic [4]. As shown in figure 2, electromagnetic shower is more localized in a material, while hadronic shower is more spatially extended. Electromagnetic showers are caused by photons and electrons. Electrons create many events in matter by ionization and bremsstrahlung, and photons are able to penetrate quite far through material before they lose energy. The second type, hadronic showers, is caused by hadrons – particles that are made of quarks - and strong nuclear forces are involved into those interactions. The hadronic showers are characterized by ionization and interactions between incident particles and nuclei of the material. Hadronic showers are complex, as many reactions take place and many different particles are produced, and it is essential to use sophisticated modelling packages such as GEANT4 [5] to understand hadronic showers.

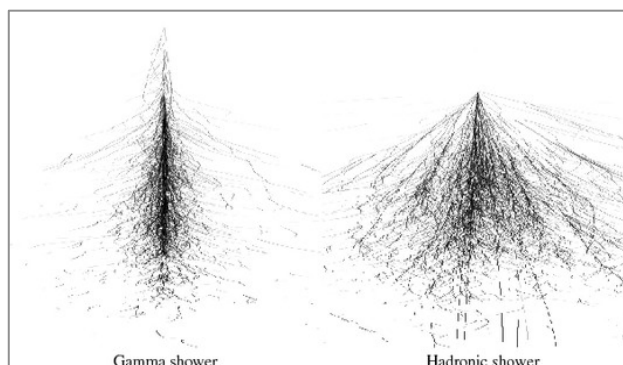


**Figure 2.** The different character of electromagnetic and hadronic showers [4].

One can distinguish two different types of showers, but typically the hadronic showers include electromagnetic processes (hadronic shower tails are electromagnetic) and both of them take place within the high energy interactions in matter. High energy particles interact with nuclei, secondary particles are produced, and these impact other particles. This process will continue until the particle energies are reduced below the thresholds for generating more secondary particles, at which point the particles are absorbed in matter.

The spatial extent of a particle shower depends on the energy of incoming particles (that dependence is logarithmic) and on the material they hit. This is why examining different materials in order to know how they can produce and/or stop particle showers is important for building a solution which will reduce high energy background.

## 2. Geant4 simulation idea

Geant4, a reliable simulation toolkit for areas where particle interactions in matter play a main role [6], was used to perform the simulations. That toolkit is a well-known main simulation engine for high energy physics applications. Different materials were investigated in order to understand their shielding properties against high energy particles. Materials studied here include iron, copper, steel, aluminium, regular concrete and tungsten. They were investigated in terms of their high energy shielding properties. The simulations involved blocks of each material of 2x2 meters (length x height), with thicknesses varying from 10 centimetres to 3 meters. The particle source in Geant4 simulations (particle gun) is placed in front of the centre of the block.  $10^6$  neutrons with energy 2.5 GeV were emitted along the z-axis, representing a fast neutron emitted with all of the proton energy at an ESS-like target station. The “perfect detector”, with a size of 2x2 meters (length x height), is placed right after the block, as shown schematically in figure 3. The “perfect detector” was used for illustrative purposes in those simulations, but for a full optimisation here the details of sensitivity of the detectors to various particle species and energy would be absolutely key. The physics list *QGSP\_BERT\_HP*, recommended for shielding applications in the energy range of interest, was chosen for the simulations. This is the set of physical processes which describe the interaction of particles with dense matter [6]. The abbreviation means the following: *QGS* is for quark-gluon string model, *P* means precompound, *BERT* means that Bertini intra-nuclear cascade model is used, and *HP* states that high precision neutron tracking model is also included [7]. The results of simulations are the types of the “surviving” particles after going through the each block and their energies. In other words, for every fast neutron interacting with the shielding block, we determine how many and what kinds of particles are transmitted to the other side, including all generated particles.

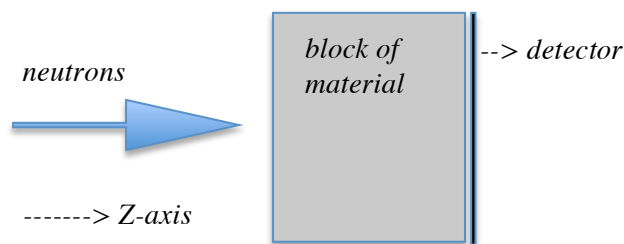


**Figure 3.** A scheme of the simulation setup

## 3. Simulations and their results

Iron, with a relatively small atomic number, was chosen for the simulations to investigate its shielding properties because iron-based materials are widely used for shielding purposes in neutron scattering facilities. The isotopic composition of iron, the default G4\_Fe material, is the following:

Fe54 ( $Z = 26$ ,  $N = 54$ ,  $A = 53.94$  g/mole), abundance = 5.84%

Fe56 ( $Z = 26, N = 56, A = 55.93$  g/mole), abundance = 91.75%

Fe57 ( $Z = 26, N = 57, A = 56.94$  g/mole), abundance = 2.12%

Fe58 ( $Z = 26, N = 58, A = 57.93$  g/mole), abundance = 0.28%

As one can see from figure 4, the number of particles developed by particle showers in iron, increases in small (up to 70 cm) blocks of iron. The particle count peak is known as “shower maximum”. Note that 50 cm of iron actually “amplifies” the background flux by 1-2 orders of magnitude. This has implications for “T0 Chopper” design at spallation sources that may not have been accounted for in their design at present generation spallation sources. After the peak, it approaches a straight line in a log-plot (or exponential in a linear plot) when the secondary particles' equilibrium is reached. We then observe that the number of particles decreases to the initial number ( $10^6$ ) of neutrons when the thickness of the block is about 180 cm. After 3 metres of iron, the number of particles is still greater than  $10^4$ ; i.e. a shielding factor corresponding to only 2 orders of magnitude. For some materials, neutrons dominate, for some other, as one can see below, the difference in number of neutrons and other particles is significant. However, we're particularly interested in neutron performance of the shielding at the moment.

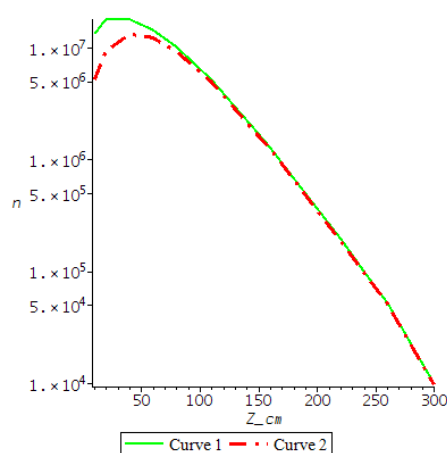


**Figure 4.** Number of particles detected in the simulation with  $10^6$  incident neutrons after initial particles are emitted into the blocks of iron as a function of thickness of the block.  $n$  is the number of particles,  $Z_{cm}$  is the thickness of the block. Curve 1 (solid) corresponds to all particles (excluding neutrinos), curve 2 (dashed) corresponds to neutrons.

Copper has been avoided on the past at neutron sources because of the cost, but we are interested in reducing the total cost of the whole shielding system. Copper has been simulated since it has very favourable shielding characteristics. As a result, copper is used in high energy physics laboratories (for example, CMS experiment in CERN [8]). Thus, we should not exclude expensive materials, which offer high performance and can be a part of solution.

The isotopic composition of copper, the default G4\_Cu material, is the following:

Cu63 ( $Z = 29, N = 63, A = 62.93$  g/mole), abundance = 69.17%

Cu65 ( $Z = 29, N = 65, A = 64.93$  g/mole), abundance = 30.83%

As one can see from figure 5, the number of particles developed by particle showers in copper has a similar qualitative shape to that of iron, but reaches the initial number ( $10^6$ ) of neutrons when the thickness of the block is about 110 cm. When it comes to blocks with thickness of blocks about 200 cm and more, the difference between iron and copper is about 2 orders of magnitude. This demonstrates the advantage of copper in stopping high energy particles in comparison with iron. (Please see also figure 7 for that comparison and also for comparison with steel, discussed below).

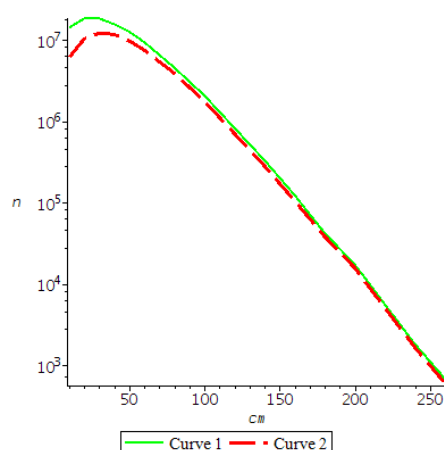


**Figure 5.** Number of particles detected in the simulation with  $10^6$  incident neutrons after initial particles are emitted into the blocks of copper as a function of thickness of the block.  $n$  is the number of particles,  $Z_{cm}$  is the thickness of the block. Curve 1 (solid) corresponds to all particles (excluding neutrinos), curve 2 (dashed) corresponds to neutrons.

Steel, as one of the widely used materials for shielding purposes, was also simulated. The type of steel that was used is carbon structural steel, which is used at SNS. It is defined in “ASTM A36 Standard Specification for Carbon Structural Steel” by American Society for Testing and Materials (CFR Section: 46 CFR 160.035-3(b)(2)).

The following composition of materials (the standard requirements for shapes of all thicknesses) was chosen: carbon, 0.26%; phosphorus, 0.04%; sulfur, 0.05%; silicon, 0.4%; copper, 0.2%; iron, 99.05%. The density of the steel is  $7.85 \text{ g/cm}^3$ . In that particular simulation, the number of neutron emitted into the block is not  $10^6$  as for all other simulations, but  $10^5$ .

As shown on the figure 6, the structural carbon steel has approximately the same behaviour as iron in terms of blocking the high energy particles, which is not surprising given that the composition is mostly iron. The number of particles developed by particle showers in steel again initially increases in a small (up to 70 cm) blocks up to shower maximum, and decreases back to the initial number ( $10^5$ ) of neutrons when the thickness of the block is about 170 cm. To see the comparison of number of neutrons as a function of thickness of the block for iron, copper and steel, refer to figure 6, where the values for steel are multiplied by order of magnitude to be within the same scale with values for iron and copper.

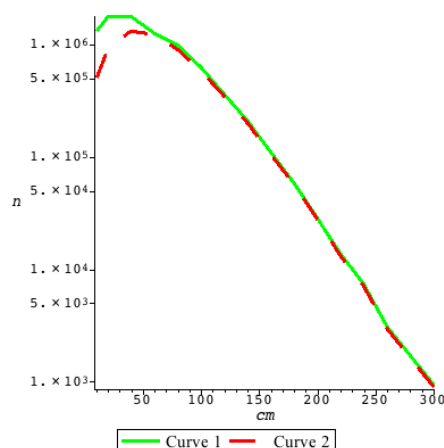


**Figure 6.** Number of particles detected in the simulation with  $10^6$  incident neutrons after initial particles are emitted into the blocks of steel as a function of thickness of the block.  $n$  is the number of particles,  $Z_{cm}$  is the thickness of the block. Curve 1 corresponds to all particles (excluding neutrinos), curve 2 corresponds to neutrons.

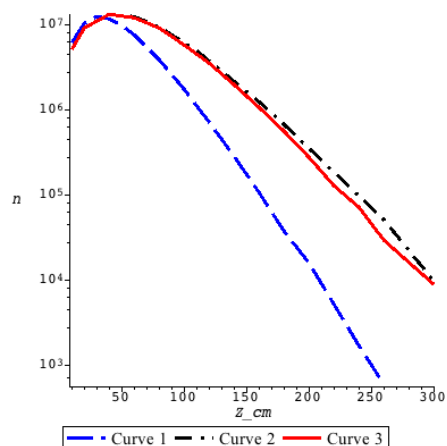


**Figure 7.** The number of neutrons which are detected in the simulation after initial particles are emitted into the blocks of copper (curve 1, long dash), iron (curve 2, dash-dot) and steel (curve 3, solid) as a function of thickness of the block. Number of incident neutrons is  $10^6$  for curve 1 and curve 2. Number of incident neutrons is  $10^5$  for curve 3 and those results are multiplied by 1 order of magnitude.  $n$  is the number of particles,  $Z_{cm}$  is the thickness of the block.

In figure 8, figure 9 and figure 10 one can see the total cross sections as a function of neutron energy in 3 materials, discussed above – iron, copper and steel, correspondingly, which illustrates the performance differences between a copper-based shielding strategy and an iron-based shielding strategy. As one can see, iron and steel are very similar in terms of nuclear resonances and windows of high transparency. Measured cross sections taken from the EXFOR/IAEA Nuclear Data Services website (<http://www-nds.iaea.org/nrdc/basics/>).

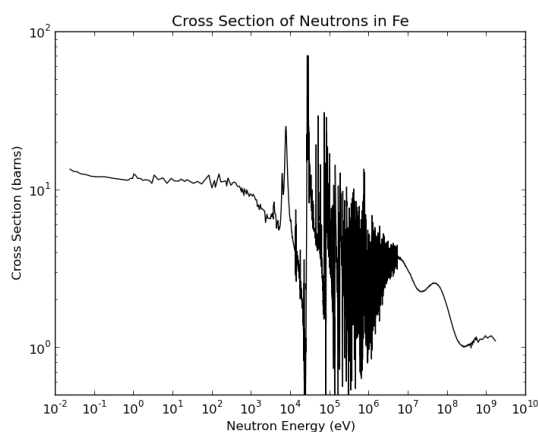


**Figure 8.** Measured total cross section of neutrons in iron as a function of neutron energy.

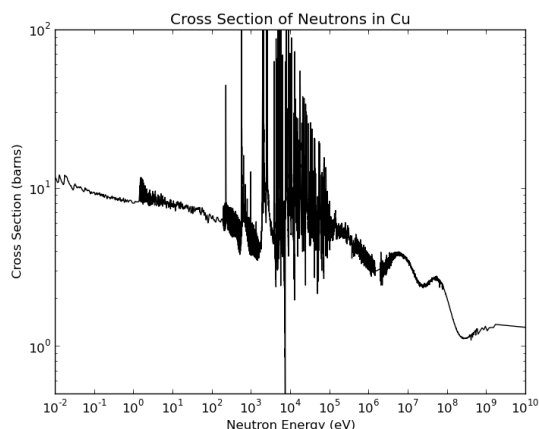


**Figure 9.** Measured total cross section of neutrons in copper as a function of neutron energy.

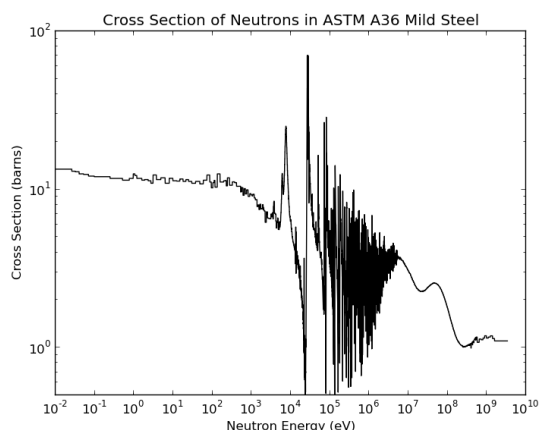


**Figure 10.** Total cross section of neutrons in steel as a function of neutron energy as a weighted combination of measured data sets for each chemical ingredient.

We have also examined aluminium, to show the behaviour of a structural material with a low atomic number compared to these of other shielding materials. The isotopic composition of aluminium, the default G4\_Al material, is the following:

Al27 ( $Z = 13$ ,  $N = 27$ ,  $A = 26.98$  g/mole), abundance = 100%

As one can expect, aluminium turns out to be less efficient in stopping high energy particles than iron. The number of particles developed by particle showers in aluminium increases in larger blocks of aluminium (up to 100 cm), and it goes down to initial number ( $10^6$ ) only when the thickness of the block is about 270 cm. Please see figure 11 where the number of particles as a function of thickness of the block is shown.

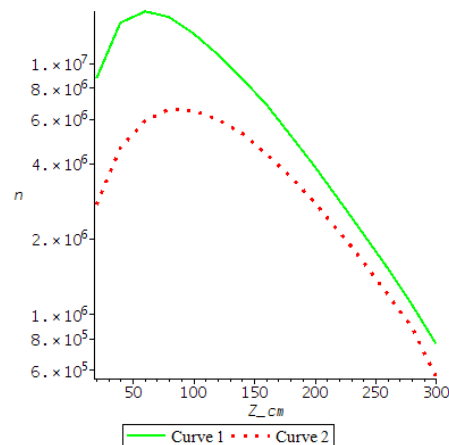


**Figure 11.** Number of particles detected in the simulation with  $10^6$  incident neutrons after initial particles are emitted into the blocks of aluminium as a function of thickness of the block.  $n$  is the number of particles,  $Z_{cm}$  is the thickness of the block. Curve 1 (solid) corresponds to all particles (excluding neutrinos), curve 2 (dashed) corresponds to neutrons.

Concrete was also studied for the simulations as very common material, well-known by its applications in different fields, including shielding purposes. The particular material, used for simulations, is regular concrete, which has a large water content that tends to be effective at moderating epithermal neutrons. The components of concrete, the default G4\_CONCRETE material, are the following: hydrogen 1%; carbon 0.01%; oxygen 52.9107%; sodium 1.6%; magnesium 0.02%; aluminum 3.3872%; silicon 33.7021%; potassium 13%; calcium 4.4%; iron 1.4%. Density of concrete is  $2.3 \text{ g/cm}^3$ .

As one can see from figure 12, even if the number of particles, created by particle showers in concrete, increases in relatively small blocks (up to 70 cm), it goes down very slowly and reaches the initial number of neutrons when the thickness of block is about 170 cm. Even with the thickness of the block about 280 cm, the number of neutrons as well as the number of all particles remains significant.

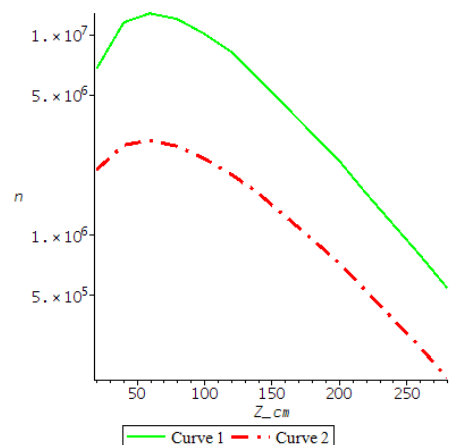


**Figure 12.** Number of particles detected in the simulation with  $10^6$  incident neutrons after initial particles are emitted into the blocks of concrete as a function of thickness of the block.  $n$  is the number of particles,  $Z_{cm}$  is the thickness of the block. Curve 1 corresponds to all particles (excluding neutrinos), curve 2 corresponds to neutrons.

Finally, tungsten has been studied for simulation as a dense, high-Z material. The isotopic composition of tungsten, the default G4\_W material, is the following:

W180 ( $Z = 74, N = 180, A = 179.95$  g/mole), abundance = 0.12%

W182 ( $Z = 74, N = 182, A = 181.95$  g/mole), abundance = 26.5%

W183 ( $Z = 74, N = 183, A = 182.95$  g/mole), abundance = 14.31%

W184 ( $Z = 74, N = 184, A = 183.95$  g/mole), abundance = 30.64%

W186 ( $Z = 74, N = 186, A = 185.95$  g/mole), abundance = 28.43%

As one can see from figure 13, the number of particles developed by particle showers in tungsten, increases in very small (about 20 cm) blocks. It goes down very quickly, reaches the initial number ( $10^6$ ) of neutrons with the thickness of the block is about 60 cm. The number of particles goes down to significantly small numbers with the thickness of tungsten block about 180 cm. Tungsten is well known to be very efficient material in stopping and adsorbing particle showers. The main drawback with tungsten is the cost so tungsten can only be used as part of the solution in key areas.

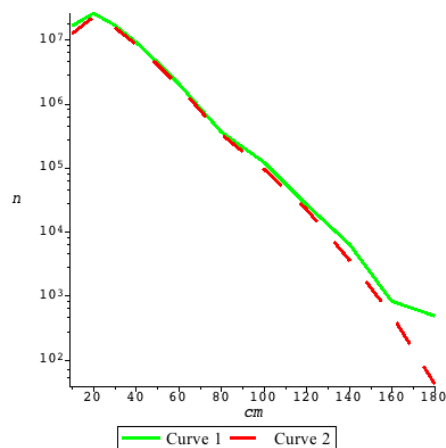


**Figure 13.** Number of particles detected in the simulation with  $10^6$  incident neutrons after initial particles are emitted into the blocks of tungsten as a function of thickness of the block.  $n$  is the number of particles,  $Z\_cm$  is the thickness of the block. Curve 1 (solid) corresponds to all particles, curve 2 (broken) corresponds to neutrons. The artefact at 160-180 cm is caused by the low statistics, due to the effectiveness of tungsten as a shielding material.

Table 1 compares the performance of these different materials in dealing specifically with GeV neutrons.

Current efforts are now investigating laminate shielding solutions, combining different materials effectively to exceed the performance of any single ingredient.

**Table 1.** The comparison of different materials and combination of materials in terms of particles (and particularly neutrons) coming through them.

Name of the material and thickness	Emerging neutrons detected, % of initial number of neutrons
<b>Iron, 3 m</b>	~ 1%
<b>Copper, 2.6 m</b>	~ 0.06%
<b>Steel, 3 m</b>	~ 0.9%
<b>Aluminium, 3 m</b>	~ 56%
<b>Concrete, 2.6 m</b>	~ 28%
<b>Tungsten, 1.6 m</b>	~ 0.05%

#### 4. Conclusions

Iron-based shielding is commonly used at spallation neutron sources, but has well-known nuclear resonances, producing windows of high transparency between 100 keV and 1 MeV. Structural carbon steel has approximately the same behavior as iron in terms of blocking high energy background, and neither can be thought of as a complete shielding solution without supplementary materials. Copper has been demonstrated at high energy physics labs in multiple roles and has superior properties compared to iron and steel; and copper-based solutions deep inside key shielding areas are seen to be attractive avenue of further research in reaching our background goals.

Tungsten is a well-known high performance shielding material, but can be only a part of the shielding solution because of its cost; we are interested in reducing the total cost of the whole shielding system. Aluminum and regular concrete are used widely in neutron instruments, and readily initiates particle showers at high energy, but do not significantly contribute to containing the subsequent shower.

#### 5. Acknowledgements

The authors wish to thank, in alphabetical order, S Ansell, K Batkov, C Cooper-Jensen, D DiJulio, K Fissum, M Fitzsimmons, S Kenney, O Kirstein, T Krist, D Martin Rodriguez, D Mildner, E Pitcher, T Sato, T Shea, L Tchelidze and L Zanini for useful discussions. Authors based at Oak Ridge acknowledge funding by the Scientific User Facilities Division, Office of Basic Energy Sciences, US Department of Energy.

#### 6. References

- [1] Russel G *et al.* 1988 Shielding concerns at a spallation source *Proceedings of the ICANS-X Conference, Los Alamos, NM*
- [2] Winn B and Hagen M 2012 Inelastic spurion from the prompt pulse [http://neutrons.phy.bnl.gov/HYSPEC/memos\\_technical\\_reports.shtml](http://neutrons.phy.bnl.gov/HYSPEC/memos_technical_reports.shtml)
- [3] HYSPEC status reports <http://neutrons.ornl.gov/hyspec/documentation/>
- [4] Gaudio G, Livan M and Wigmans R 2009 *Proceedings of the International School of Physics "Enrico Fermi"* 175 31-77
- [5] Völk H and Bernlöhr K 2009 *Exp. Astr.* **25** (1-3) 173-191
- [6] Agostinelli S *et al.* 2003 *Nucl. Instrum. and Methods in Phys. Res. A* **506** 250-303
- [7] Speckmayer P 2010 Impact of the choice of physics list on GEANT4 simulations of hadronic showers in tungsten LCD-Note-2010-002
- [8] CMS collaboration 2008 *JINST* S08004